J Electr Eng Technol.2018; 13(?): 1921-718
http://doi.org/10.???/JEET.2018.13.1.1921

ISSN(Print) 1975-0102
ISSN(Online) 2093-7423

Vibration Analysis of Transformer DC bias Caused by HVDC based on EMD Reconstruction

Xingmou Liu†, Yongming Yang* and Yichen Huang**

Abstract – This paper proposes a new approach utilizing empirical mode decomposition (EMD) reconstruction to process vibration signals of a transformer under DC bias caused by high voltage direction transmission (HVDC), which is the potential cause of additional vibration and noise from transformer. Firstly, the Calculation Method is presented and a 3D model of transformer is simulated to analyze transformer deformation characteristic and the result indicate the main vibration is produced along axial direction of three core limbs. Vibration test system has been built and test points on the core and shell of transformer have been measured. Then, the signal reconstruction method for transformer vibration based on EMD is proposed. Through the EMD decomposition, the corrupted noise can be selectively reconstructed by the certain frequency IMFs and better vibration signals of transformer have been obtained. After EMD reconstruction, the vibrations are compared between transformer in normal work and with DC bias. When DC bias occurs, odd harmonics, vibration of core and shell, behave as a nonlinear increase and the even harmonics keep unchanged with DC current. Experiment results are provided to collaborate our theoretical analysis and to illustrate the effectiveness of the proposed EMD method.

Keywords: Transformer vibration, HVDC transmission, Signal reconstruction, EMD

1. Introduction

The energy internet has been proposed and will be developed all over the world, which leads to more and more high voltage DC transmission (HVDC) systems are utilized since they can increase power transmission capacity, provide high stability for long-distance power delivery, but HVDC also creates some problems in grid. When the monopole mode is operated HVDC system, as shown in Fig. 1, DC current produced from converter in the power circuit flows into the neutral grounding of ac power transformer nearby HVDC [1]. However, the DC current will lead to transformer core saturation and moves out of the magnetization linear operation region, increase exciting current distortion, loss increase and abnormal vibration [2]. DC bias problem is studied in theory and the mode under DC bias based on electric and magnetic circuit theory is proposed in [3, 4] . The simulation explaining saturation phenomena of transformer core is researched in [5] and [6]. Then, the key of transformer core vibration is material magnetostriction [7]. Regarding the relation between magnetostriction and vibration, an investigation is performed with experiments that including vibration measurements in [8, 9]. And some research focus on the vibration analysis and knowledge acquisition for feature extraction [10-13]. However, diagnosing transformers with vibration methods for DC bias is a new area, so few related research has been conducted.

Actually, the DC bias problem mainly inflences the distribution transformers, which have high power capacity and are made of core type. However, the shell type transformers are usually used for low capacity transmission of power, such as domestic appliances. Thus, the DC bias vibration of shell type transformers are not considered in this research.

In this paper, a new method combined empirical mode decomposition (EMD) is presented for transformer vibration analysis influenced by DC bias. EMD can adaptively decompose the vibration signals without any restriction. Because it does not impose priori assumptions to the data [14]. The signal is decomposed into a sequence of intrinsic mode functions (IMFs) and a residue with different frequency band [15]. So that it is suitable for separating the noise

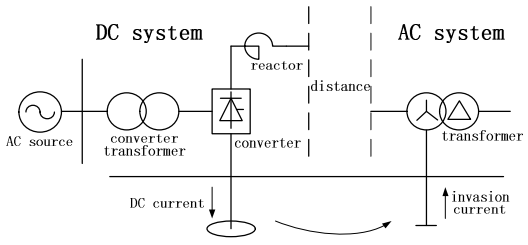

Fig. 1. Process of transformer DC bias caused by HVDC

† Corresponding Author: College of Automation, Chongqing University of Posts and Telecommunications, Chongqing, China (liuxingmou@cqu.edu.cn)
* School of Electrical Engineering, Chongqing University, Chongqing, China. (yangyym@cqu.edu.cn)
** State Grid Jiangxi Economic Research Institute, Nanchang, Jiangxi, China. (huangyichen1005@126.com)
Received: May 22, 2017; Accepted: November 15, 2017

modes using EMD method. The significant contribution of this research is the vibration signal reconstruction based on EMD. Firstly, a 3D model calculation and simulation are performed to analyze transformer deformation characteristic and determine test location. Then, the principle and calculation process of EMD have been presented. Meanwhile, the DC bias experiment on the three-phase 5kVA transformer is carried on and the vibration signals of five different points on core and shell are monitored. The test signals must contain a large amount of interference and noise which is caused by test system and environment. According to the feature of transformer noise, the interference modes of transformer vibration are filtered through EMD reconstruction so that to obtain the effective vibration signals. In addition, the harmonics characteristic of vibration signals have been analyzed through reconstructed signals. Result shows the odd harmonics increased obviously as a linear characteristic but even harmonics almost remain unchanged with the increase of DC bias, because that the silicon steel entered into saturation region by the influence of DC current. Therefore, the vibration analysis using EMD reconstruction can be a good method to extract the useful components of transformer vibration. This research also demonstrates that DC bias of transformer is remarkable and it must be considered for transformer design and its applications.

2. Transformer Deformation Calculation

2.1 Mathematical model for transformer deformation

Transformer vibration is mainly caused by the magneto-striction of silicon steel and electromagnetic force of core. In this research, we calculated the force and displacement of a no-load transformer core by building a 3-D magnetic force model. Based on the Maxwell equations and magnetic vector potential equation, the electromagnetic equation can be expressed as follow [16]

$$\left(\nabla\cdot\frac{1}{\mu}\nabla\right)A=-J_s+j\omega\sigma A \tag{1}$$

among B=▽×A and B=μH. Where μ is the permeability; B is the magnetic flux; H is the magnetic field; A is the magnetic vector potential; σ is the conductivity; J_s is the applied current density; ω is the angular frequency.

Magnetostriction is the intrinsic property of silicon steel that can be expressed by the following piezomagnetic equation in tensor form [17]:

$$\begin{cases}\varepsilon_p=\sum_{q=1}^{6}s_{pq}^{H}\sigma_p+\sum_{m=1}^{3}d_{mp}H_m & p=1,2,\cdots,6\\ B_n=\sum_{q=1}^{6}d_{nq}\sigma_q+\sum_{m=1}^{3}\mu_{nm}^{\sigma}H_n & n=1,2,3\end{cases} \tag{2}$$

Where s^H, d, and μ^σ are the elastic constants in the constant magnetic field, the magnetostriction coefficient, and the permeability in constant stress, respectively. ε_p and σ_p are the strain and stress tensor components. B_n and H_n are the magnetic flux density and magnetic vectors, respectively.

The total energy of transformer cores comprises strain energy, magnetic energy, magnetostriction energy, potential energy of external force, and potential energy of current [18]. On the basis of constitutive relations (2), the following energy function of the analysis system is developed [19]:

$$\begin{aligned}I=&\int_{\Omega_2}\left(\frac{1}{2}\sigma^T\boldsymbol{s}^H\sigma\right)\mathrm{d}V+\int_{\Omega_2}\left(\sigma^T d\boldsymbol{H}\right)\mathrm{d}V\\&+\int_{\Omega_1}\left(\frac{1}{2}\boldsymbol{H}^T\mu^\sigma\boldsymbol{H}\right)\mathrm{d}V-\int_{\Omega_1}\boldsymbol{J}\cdot\boldsymbol{A}\mathrm{d}V\end{aligned} \tag{3}$$

Among A, defined by B=▽×A, is the magnetic vector potential; u is the distortion of transformer core; J is the external current density; and Ω_1 and Ω_2 are the analysis regions of the magnetic field and the machine, respectively. $\int_{\Omega_1}\left(\frac{1}{2}\boldsymbol{H}^T\mu^\sigma\boldsymbol{H}\right)\mathrm{d}V$ means magnetic energy; $\int_{\Omega_1}\boldsymbol{J}\cdot\boldsymbol{A}\mathrm{d}V$ means the potential energy of current; $\int_{\Omega_2}\left(\frac{1}{2}\sigma^T\boldsymbol{s}^H\sigma\right)\mathrm{d}V$ means mechanical energy; $\int_{\Omega_2}\left(\sigma^T d\boldsymbol{H}\right)\mathrm{d}V$ means magneto-mechanical energy; $\int_{\Omega_2}\left(\sigma^T d\boldsymbol{H}\right)\mathrm{d}V$ means the coupling energy of magneto-mechanical [20]. The 3D coupling energy analysis of strain of silicon steel can be expressed by

$$\begin{aligned}&\int_{\Omega_2}\left(\sigma^T d\boldsymbol{H}\right)\mathrm{d}V=E^\alpha\int_{\Omega_2}\{Z\}\mathrm{d}x\mathrm{d}y\mathrm{d}z\\&Z=\begin{bmatrix}(1-\alpha)\varepsilon_x+\alpha\varepsilon_y+\alpha\varepsilon_z\\ \alpha\varepsilon_x+(1-\alpha)\varepsilon_y+\alpha\varepsilon_z\\ \alpha\varepsilon_x+\alpha\varepsilon_y+(1-\alpha)\varepsilon_z\end{bmatrix}^T\begin{bmatrix}d_{11}&d_{12}&d_{13}\\ d_{21}&d_{22}&d_{23}\\ d_{31}&d_{32}&d_{33}\end{bmatrix}\begin{bmatrix}H_x\\ H_y\\ H_z\end{bmatrix}\end{aligned} \tag{4}$$

$$E^\alpha=\frac{E}{(1+\alpha)(1-2\alpha)} \tag{5}$$

Among α is the Poisson ratio, E is the Young's modulus. d_{11},d_{22},d_{33} can be obtained from measured magnetostriction curve. Getting $d_{21}=d_{31}=-\alpha d_{11}$, $d_{12}=d_{32}=-\alpha d_{22}$, $d_{13}=d_{23}=-\alpha d_{33}$, through the Hooker's law.

After element discretization of functional and element assembly, then the matrix equation of the magneto-mechanical couplingcan be expressed as

$$\begin{pmatrix}M&D\\ C&K\end{pmatrix}\begin{pmatrix}A\\ u\end{pmatrix}=\begin{pmatrix}J\\ 0\end{pmatrix} \tag{6}$$

Table 1. SG-5 transformer parameters

nominal voltage	400V	rated capacity	5kVA
no-load current	12%	no-load loss	75W
short-circuit loss	160W	impedance voltage	3.5%

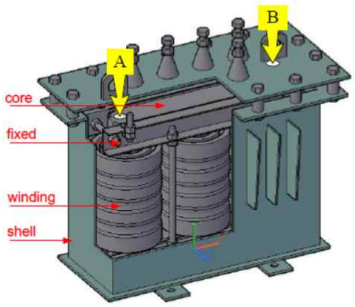

Fig. 2. Transformer model and vibration test points

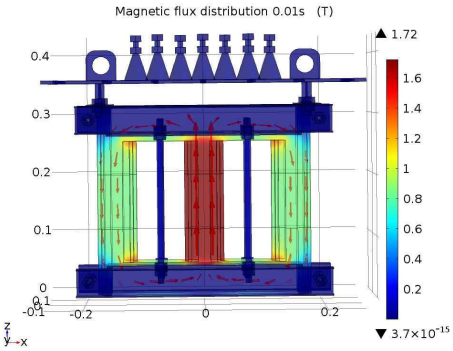

Fig. 3. Magnetic flux density distribution of transformer

Among K represents the mechanical stiffness matrix, M represents the electromagnetic matrix, C and D are satisfied with $C=D^T$. They represent the coupling interactions between the magnetic field and mechanical deformation. The magneto-mechanical coupling between magnetic field and mechanical field are strong and directly.

2.2 Calculation result and test points selection

All three-phase three-column core type transformers are designed and manufactured with the same structures. The vibraitons on same locations of different capacity transfomers have the samilar waves and frequency configuration. But the high frequency components of large power transformers are more plentiful than that of smaller transformers. This phenomenon is caused by the complex structures in big transformers [3]. Therefore, the main information of vibration in different three-phase three-column core type transformers are not influenced by the capacity and size. In order to get the convenience of this experiment, A dry, three-phase unit (5 kVA, 50 Hz) transformer is proposed for research, as shown in Fig. 2. Table 1 shows the parameters of the transformer. The full-size 3D model of the transformer under rated conditon and dc DC bias are built in COMSOL for analysis.

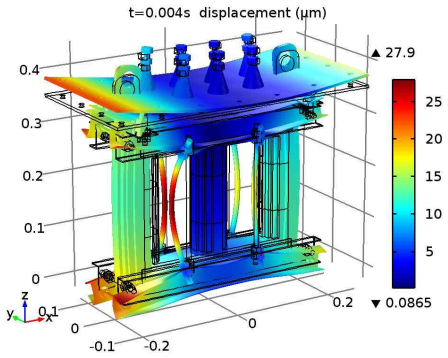

(a) Transformer displacement at 0.004s

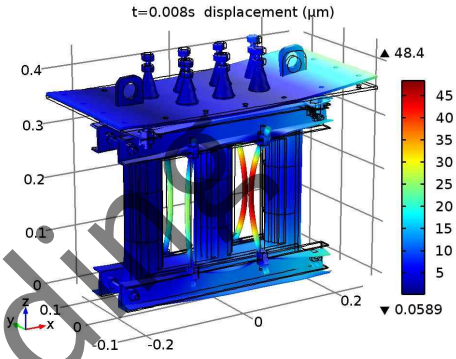

(b) Transformer displacement at 0.008s

Fig. 4. Transformer structure deformations

Fig. 4 shows transformer deformation distributions of two times (4, 8 ms) from transient FE simulation when the transformer works with rated frequency 50 Hz and considering magnetostriction and DC bias. All deformation graphics are magnified 1000 times for more clear visualization.

The deformations of fixed links and transformer shell are obvious and the maximum reached 48.4 μm on the fixed rods. According to the simulation results, it is obvious that the core corners have the most serious effect with magnetic field circuit. Meanwhile, the left and right phasse of core limbs have the largest deformation. It is because the highest magnetic field flows into both sides phase and strain caused by magnetostriction is produced maximum at the moment. So, the corner deformation could be important concerned object for researching transformer vibration caused by core magnetostriction. In order to more accurately reflect the transformer vibration, the points A and B (marked in Fig. 2) on core and shell are selected as test objects to analyze the vibration change with and without DC bias.

3. Vibration Test and Analysis

Vibration analysis of transformer is researched through experiment tests. The piezoelectricity acceleration sensors are used to measure vibration acceleration of transformer

Table 2. IC piezoelectric acceleration sensor

Sensitivity mV/g	Range g	Frequency Hz(±10%)	Resonant kHz	Resolution g
1000	5	0.1-2000	7.5	0.00002

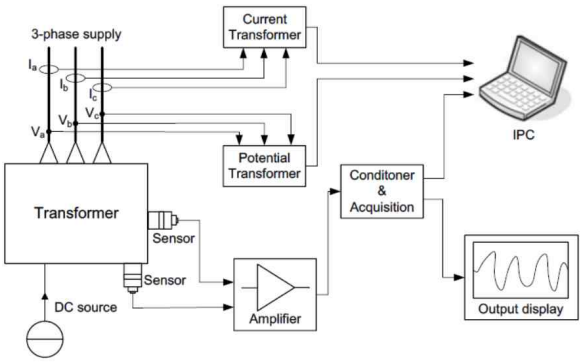

Fig. 5. The block diagram of test system

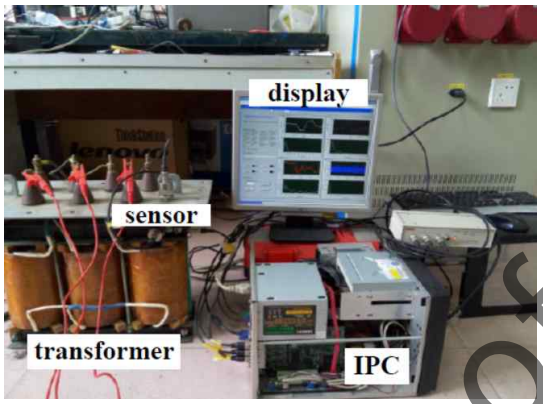

Fig. 6. Experimental system for vibration measurement

core. Its performance is as shown in Table 2. The measured signals are saved by acquisition card after amplified and conditioned. Then the signals are analyzed by an industrial personal computer (IPC). The block diagram is shown in Fig. 5 and the experimental system is shown in Fig. 6.

The transformer which is the same with the simulation one is tested and its parameters is shown in Table 2. During the test, the sensors are fixed on the core and shell. The locations of the test points are shown in Fig. 1. The first step of the test is to measure the vibrations under normal condition using the no-load test. Then, different DC current input into neutral point of transformer, and the test performed. Fig. 7 and Fig. 8 show the vibration signals of core and shell at points A and B under normal work and 2A DC current, respectively. It is obvious that the high frequency components of test waveform are more plentiful than simulation waveform. This can be explained by the noise of test and structures.

Fig. 7 and Fig. 8 show the vertical vibrations of A and B points under normal work and 2 A dc current, respectively. The vibrations are almost even harmonics such as 100 Hz,

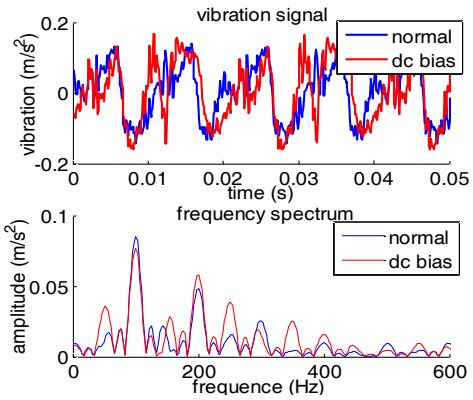

Fig. 7. Measured vibration at point A

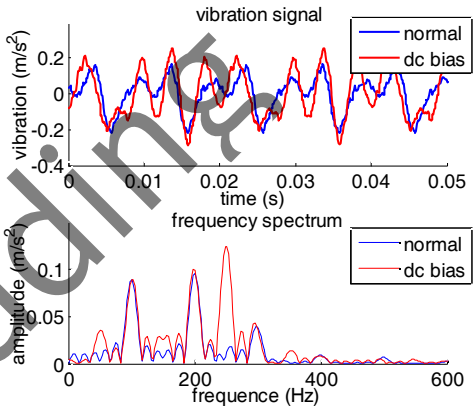

Fig. 8. Measured vibration at point B

200 Hz and 300 Hz under normal work. Relatively higher frequency components usually show the signal mingled with the noise. However, when the DC magnetic bias produced in transformer, the vibrations contain other odd harmonics such as 50 Hz, 150 Hz, and 250 Hz and so on. high frequencies change irregularly with DC bias increasing, it can be considered that the mixed results of vibration signals and noise.

4. EMD Reconstriction and Result Analysis

4.1 Empirical mode decomposition calculation

EMD is a multiresolution decomposition way that disposes the nonstationary and nonlinear signals into many IMFs that originated from analyzed signal itself. But the IMF must be satisfied two conditions [21, 22].

1) The number of extrema and zero-crossings are differ by at most one or either equal to each other.

2) At any point, the mean value between the local maximums envelope and the local minimums envelope is zero.

The EMD could be described and expressed into IMFs by the process following [23]:

1. The analyzed signal x(t), find the all local maximums and minimums then fit them into envelopes of $x_{max}(t)$ and $x_{min}(t)$ by cubic spline, respectively.

2. the mean of two envelopes can be got as:

$$m_1(t) = \left[x_{\max}(t) + x_{\min}(t)\right] / 2 \tag{7}$$

3. Compute the difference between x(t) and $m_1(t)$, the result is record as $h_1(t)$:

$$h_1(t) = x(t) - m_1(t) \tag{8}$$

4. To judge the result $h_1(t)$ whether accord with the two conditions of IMF. If accord, record $c_1(t)=h_1(t)$, and it is the first IMF component. If not, treat $h_1(t)$ as analyzed signal and iteration on $h_1(t)$ by steps 1 to 4.

5. Through the k times iteration, the difference between the original signal and the mean envelope could be defined as $h_{1k}(t)$:

$$h_{1k}(t) = h_{1(k-1)}(t) - m_{1k}(t) \tag{9}$$

where $m_{1k}(t)$ represents mean value of envelope after k times iteration and $h_{1(k-1)}(t)$ represents the difference between signal and mean of iteration. If the $h_{1k}(t)$ satisfies the IMF condition, it is recorded as $c_1(t)=h_{1k}(t)$.

6. The residue is expressed as

$$r_1(t) = x(t) - c_1(t) \tag{10}$$

Then, the $r_1(t)$ can be regard as a new signal, and iterate repeatedly to get the other IMFs according to step 1 to 5. And obtain $c_n(t)$ and a residue $r_n(t)$.

$$\begin{cases} r_1(t) = c_2(t) - r_2(t) \\ \quad \vdots \\ r_{n-1}(t) = c_n(t) - r_n(t) \end{cases} \tag{11}$$

Therefore, the x(t) can be expressed as

$$x(t) = \sum_{j=1}^{n} c_j(t) + r_n(t) \tag{12}$$

where $c_j(t)$ represents the jth IMF, $r_n(t)$ represents the residue.

However, it is impossible that each signal satisfies the two IMF conditions perfectly. The iteration stop condition can be considered as:

$$\sum_{t=0}^{T} \left[\frac{\left| h_{1(k-1)}(t) - h_{1k}(t) \right|^2}{h_{1(k-1)}^2(t)} \right] < SD \tag{13}$$

where SD is the standard deviation, and usually it can be controlled between 0.2 and 0.3. Then, it is the complete express of EMD process and the Eq. (12) shows signal is expressed by IMFs superposition.

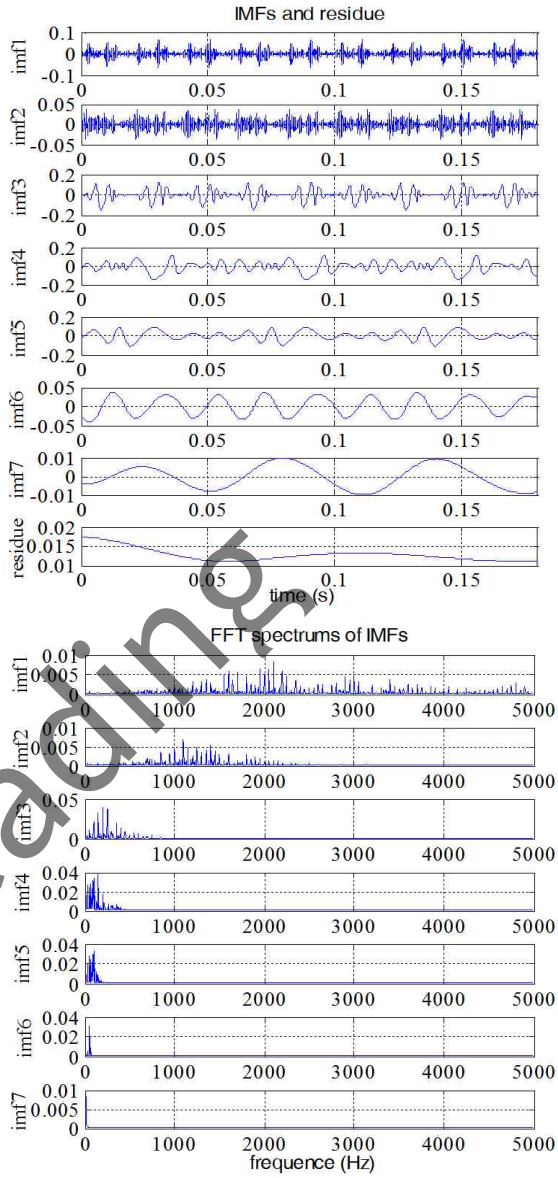

Fig. 9. Vibration decompositions of point A with DC bias by EMD

4.2 Vibration signals and EMD reconstruction

The measurement signals of point A and B are mixed with some noise of higher frequency as mentioned before. Therefore, to decompose the DC bias signal of A test point by EMD, as shown in Fig. 9.

In Fig. 9, the vibration signal is decomposed by EMD and Seven IMF components and a residue function are formed. The amplitudes of IMF1 and IMF2 are too small, i.e., approximately 10^{-3} magnitude. The main frequency range of IMF1 is approximately 1000 Hz to 5000 Hz, and the main frequency range of IMF2 is approximately 1000

Hz to 2000 Hz. These results indicate interference or noise. IMF3 to IMF7 present the intrinsic modes of the vibration signal. EMD filtrate the signal and obtained intrinsic modes from high frequency to low frequency. IMF3-IMF5 shows that the amplitude of the mid-frequency components which are main components of this signal. However, IMF6 and IMF7 indicate the low frequency modes are small. Therefore, each mode of vibration should be investigated through IMF performance. The frequency of transformer vibration is mainly concentrated in less than 1000 Hz [24].

The same method is adopted to deal with the signals of other test points. Because of the limitation of space, the IMFs waves are not displayed in paper. In order to analyze the influence of IMFs, the correlation coefficient is proprosed to obtain the relation between each IMF and original signal. According to Eq. (14), the covariance $\mathrm{cov}(c_i, x)$ is expressed through the expectations $E(x)$, $E(c_i)$ and $E(c_i \cdot x)$. Then, correlation coefficient $\rho(c_i, x)$ of each IMF and original signal could be calculated by Eq. (15).

$$\mathrm{cov}(c_i, x) = E(c_i \cdot x) - E(c_i) \cdot E(x) \tag{14}$$

$$\rho(c_i, x) = \frac{\mathrm{cov}(c_i, x)}{\sqrt{D(c_i)} \cdot \sqrt{D(x)}} \tag{15}$$

As shown in Table 3, the correlation coefficients reflect the statistical relation of similar degree between IMF obained by EMD and test signal. The results show that the IMF number of each signal depends on complexity of vibration modes may be different. However, the most relevant modes almost focus on middle IMFs: IMF5 reaches 0.7035 and IMF3 reaches 0.6727 respectively in normal and DC bias on point A; IMF4 reaches 0.6506 and IMF3 reaches 0.7928 respectively in normal and DC bias on point B. And the correlation coefficients are to reduce gradually on both sides. The correlation coefficients of residues are the minimum in each signal because the residue just indicates the monotonicity of original signal. These results further illustrates that middle modes are the main components of vibration signal.

On the other hand, the contributing rate of variance F, as shown in Eq Eq. (16), is presented to research the effective proportion of each IMF in test signal. Among $D(c_i)$ is the variance of IMF_i. The contributing rate of variance of IMFs are computed and drawn into column diagram as shown in Fig. 10. In addition, the center frequency of IMFs are extracted and the result is in Table 4.

$$F = \frac{D(c_i)}{\sum_{i=1}^{j} D(c_i)} \times 100\% \tag{16}$$

It is obvious that the contributing rates of variance of vibration signals are distributed as similar as correlation of each IMF. The high frequency components, such as IMF1 to IMF3, and the low frequency components, such as IMF7 to IMF9, often are less than 10%. This explains some modes of too high or too low almost have no effect on the signals. In shadow area of Fig. 10, the largest contributing rates of the four signals reach 62.62% of IMF5, 35.70% of IMF4, 46.43% of IMF5 and 62.27% of IMF3, respectively. And the adjoining IMFs of them also have relatively high percentages. Therefore, the main components are composed of mode series which have high contributing rates.

And then, combining the center frequency of each IMF, as shown in Table 4, to discover the useless modes and improve the signal quality. Transformer vibration is almostly consist of multifold harmonics of 50 Hz, and they mainly keep among the range of 1000 Hz [21]. Therefore, the modes which have too high center frequency can be

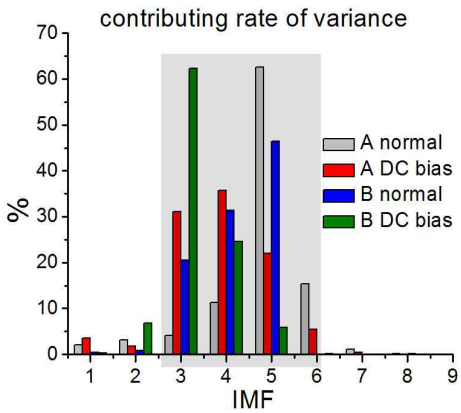

Fig. 10. Contributing rate of variance of IMFs

Table 3. Correlation coefficient of each IMF

EMD component	Point A		Point B	
	Normal	DC bias	Normal	DC bias
IMF1	0.2028	0.2167	0.1004	0.0633
IMF2	0.1971	0.1629	0.0674	0.2688
IMF3	0.1943	0.6727	0.5899	0.7928
IMF4	0.3704	0.4084	0.6506	0.4607
IMF5	0.7035	0.2787	0.6349	0.1664
IMF6	0.2825	0.2531	0.0486	0.0020
IMF7	0.0019	0.0004	0.0298	0.0008
IMF8	-0.0159	-	0.0218	-
IMF9	-0.0159	-	-	-
Residue	-0.0178	-0.0025	0.0395	0.0020

Table 4. Center frequency of each IMF (Hz)

EMD component	Point A		Point B	
	Normal	DC bias	Normal	DC bias
IMF1	3000	3150	3739	4750
IMF2	1400	1411	1439	1139
IMF3	583	277	266	205
IMF4	208	211	154	111
IMF5	136	102	100	68
IMF6	77	62	68	36
IMF7	38	17	38	19
IMF8	16	-	17	-
IMF9	6	-	-	-

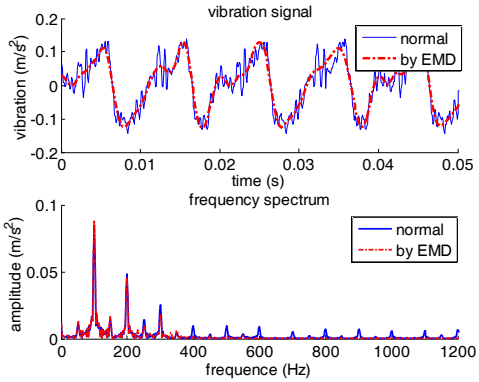

Fig. 11. Normal vibration of point A disposed by EMD

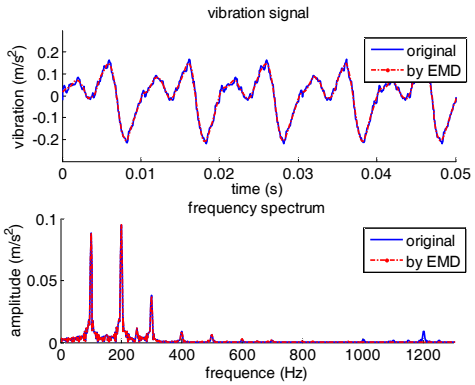

Fig. 13. Normal vibration of point B disposed by EMD

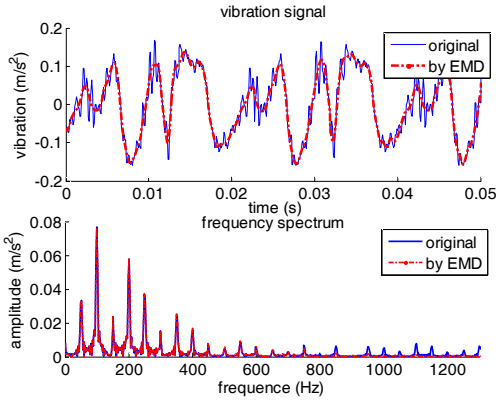

Fig. 12. DC bias vibration of point A disposed by EMD

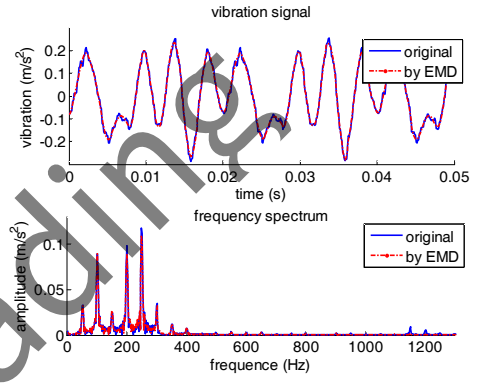

Fig. 14. DC bias vibration of point B disposed by EMD

considered as noise.

Although too low frequency may be system interference of equipment self, the amplitude of low frequecy components, such as IMF7 to IMF9, are very small. And their frequecy are more less than power frequency 50 Hz. They have a little effects on the whole signal situation.

Because the IMFs exist themself without any interacting each other. To remove the IMFs of high center frequecy more than 1000 Hz and contributing rates of variance less than 10% and reconstruct the signal by remaining IMFs. Thus, the IMF1 to IMF3 of signal on point A without DC bias and the IMF1 to IMF2 of other signals in this test need to be eliminated. The reconstruction signal are obtained as shown in Fig. 11 to Fig. 14.

After filtering some certain IMFs, the signal performance is obviously improved. The spectrum shows the high frequency of more than 1000 Hz are weakened through EMD filtering. This is different from the traditional low-pass filter. Because vibration signal is composed of the modes, and traditional low-pass filter just can recognizes the specified frequency but not modes. The EMD not only identifies the noise frequency, but also the modes of vibration. Therefore, the EMD filtering is an effective method for vibration signals.

Fig. 11 to Fig. 14 show the EMD reconstruction are effective and can perfectly remove the noise and effective components of vibration signals are enhanced. Because a series of IMFs can be separated out by EMD method from the original signal, it is a adaptive and total decompsition processing based on the vibration mode of signal. so the EMD can reconstruct selctively the effective signal on the basis of corrupted noise and certain frequency IMFs.

4.3 Vibration characteristic by DC bias

In order to investigate the each harmonic change with DC bias, the vibration signals are measured with the increasing of DC current. The optimized signals are obtained through EMD filtering. The amplitude relations between harmonic and fundamental frequency (Hz) changed are shown in Fig. 15 and 16. The abscissa represents DC current and ordinate represents harmonic amplitude ratio between DC bias and normal condition, respectively. As it can be seen from Fig. 15, amplitude ratios of odd harmonics of core vibration increased with DC current increasing. The 7th harmonic (350 Hz) component is the most obvious. When the DC current reaches 2A, it increases up to 5 times. While even harmonics almost remain unchanged. Fig. 16 shows the harmonic amplitude ratios of shell vibration, the odd harmonics increased obviously and even harmonics almost remain unchanged as well as that of core. And the 1st harmonic (50 Hz)

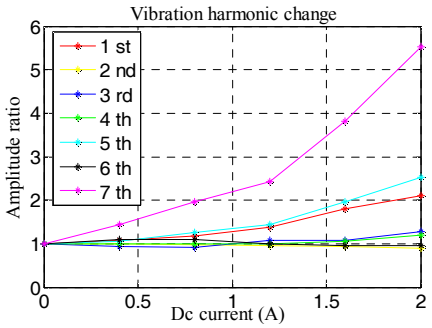

Fig. 15. Harmonic changing of point A

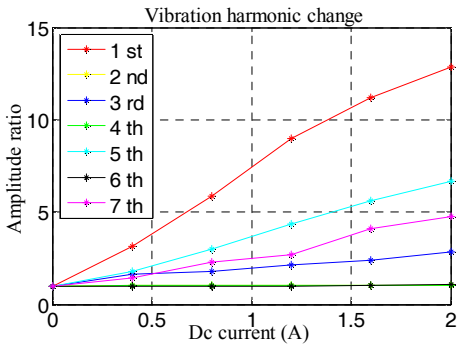

Fig. 16. Harmonic changing of point B

component increased up to 15 times. These experimental results demonstrates that the silicon steel is saturated and in a severe condition under DC bias.

It indicates that the silicon steel entered into saturation region by the influence of DC current. And magnetic flux density and magnetostriction in the saturated zone exists obvious nonlinear relationship. Therefore odd harmonics appear and increase obviously with DC current.

5. Conclusion

This paper proposes a new method for vibration signal filtering based on EMD is proposed. The EMD method could adaptively separate the original signal into a series of IMFs. Then, a 3D model calculation is performed to analyze transformer deformation characteristic and the result indicate the main vibration is produced along axial direction of three core limbs. A vibration test system has been built and test points on the core and shell of transformer have been measured. Through the EMD decomposition, the corrupted noise can be selectively reconstructed by the certain frequency IMFs. Thereby better vibration signals of transformer have been obtained. After EMD reconstruction, the vibrations are compared between transformer in normal work and with DC bias. The result shows that the harmonic vibration is related to the DC bias condition. When DC bias occurs, odd harmonics, vibration of core and shell, behave as a nonlinear increase and the even harmonics keep unchanged with DC current. The EMD reconstruction method is proved effectively to analyze the vibration signal of transformer. Meanwhile, DC bias of transformer is remarkable and they must be considered for transformer design and its applications.

Acknowledgements

The work are financially supported by National Natural Science Foundation of China Project (51247008), Scientific Research Foundation of State Key Lab of Power Transmission Equipment and System Security (2007DA10512713208) and Innovation Team Project of Chongqing Education Committee(CXTDX201601019).

References

[1] B. Zhang, X. Cui, R. Zeng and J. He, "Calculation of DC current distribution in AC power system near HVDC system by using moment method coupled to circuit equations," *IEEE Transactions on Magnetics*, vol. 6, no. 55, pp. 703-706, 2016.

[2] Yang Y, Liu X, Chen T, et al. "Impact of soil structure adjacent to ground electrodes of UHVDC power transmission lines on DC bias of power transformers," *Power System Technology*, vol. 36, no. 7, pp. 26-32, 2012.

[3] Wang J, Gao C, Duan X, et al. "Multi-field Coupling Simulation and Experimental Study on Transformer Vibration Caused by DC Bias," *Journal of Electrical Engineering & Technology*, vol. 10, no. 1, pp. 176-187, 2015.

[4] Ahn H M, Kim J K, Oh Y H, et al. "Multi-physics Analysis for Temperature Rise Prediction of Power Transformer," *Journal of Electrical Engineering & Technology*, vol. 9, no. 1, pp. 114-120, 2014.

[5] M. Dolinar, D. Dolinar, G. Stumberger, B. Polajzer, and J. Ritonja, "A three-phase core-type transformer iron core model with included magnetic cross saturation," *IEEE Transactions on Magnetics*, vol. 42, no. 10, pp. 2849-2851, 2006.

[6] Cho S D. "Three-phase Transformer Model and Parameter Estimation for ATP," *Journal of Electrical Engineering & Technology*, vol. 1, no. 3, pp. 302-307, 2006.

[7] Q. Li, X. Wang, L. Zhang, J. Lou, L. Zou, "Modelling methodology for transformer core vibrations based on the magnetostrictive properties," *IET Electric Power Applications*, vol. 6, no. 9, pp. 604-610, 2012.

[8] A. J. Moses, "Measurement of magnetostriction and vibration with regard to transformer noise," *IEEE Transactions on Magnetics*, vol. 10, no. 2, pp. 154-156, 1997.

[9] T. Nakase, M. Nakano, F.N. Takahashi, "Measuring system for magnetostriction of silicon steel sheet

under AC excitation using optical methods," *IEEE Transactions on Magnetics*, vol. 34, no. 4, pp. 2072-2074, 1998.
[10] S Y Wu, W G Huang, F R Kong. "Vibration features extraction of power transformer using all time-scale-frequency analysis method based on WPT and HHT," *IEEE 6th International Power Electronics and Motion Control Conference*, 2009.
[11] S C Ji, Y F Luo, Y M Li, "Research on extraction technique of transformer core fundamental frequency vibration based on OLTC," *IEEE Transactions on Power Delivery*, vol. 21, no. 4, pp. 1981-1988, 2006.
[12] C. Bartoletti, M. Desiderio, D.D. Carlo, "Vibro-Acoustic techniques to diagnose power transformers," *IEEE Transactions on Power Delivery*, vol. 19, no. 1, pp. 221-229, 2004.
[13] Abeywickrama N, Ekanayake C, Serdyuk Y V, et al. "Effects of the Insulation Quality on the Frequency Response of Power Transformers," *Journal of Electrical Engineering & Technology*, vol. 1, no. 4, pp. 534-542, 2006.
[14] He Lifang, Cao Li, Zhang Tianqi. "Stochastic resonance research with EMD de-noising under Levy noise," *Journal of Electronic Measurement and Instrumentation*, vol. 31, no. 1, pp. 21- 28, 2017.
[15] F. Zhou, L. Yang, H. Zhou, L. Yang, "Optimal averages for nonlinear signal decompositions-another alternative for empirical mode decomposition," *Signal Processing*, vol. 121, pp. 17-29, 2016.
[16] J. Jang, Y. Chiu, "Numerical and experimental thermal analysis for a metallic hollow cylinder subjected to step-wise electro-magnetic induction heating," *Applied Thermal Engineering*, vol. 27, pp. 883-1894, 2007.
[17] M. Dolinar, D. Dolinar, G. Stumberger, B. Polajzer and J. Ritonja, "A three-phase core-type transformer iron core model with included magnetic cross saturation," *IEEE Transactions on Magnetics*, vol. 42, no. 10, pp. 2849- 2851, 2006.
[18] F. Claeyssen, N. Lhermet, R. Le Letty and P. Bouchilloux, "Actuators, transducers and motors based on giant magnetostriction materials," *Journal of Alloys and Compounds*, vol. 258, no. 1/2, pp. 61-73, 1997.
[19] H. Shin, J. Choi, H. Park and S. Jang, "Vibration analysis and measurements through prediction of electromagnetic vibration sources of permanent magnet synchronous motor based on analytical magnetic field calculations," *IEEE Transactions on Magnetics*, vol. 48, no. 11, pp. 4216-4219, 2012.
[20] R. Yan, B. Wang, Q. Yang, F. Liu, S. Cao and W. Huang, "A numerical model of displacement for giant magnetostrictive actuator," *IEEE Transactions on Applied Superconductivity*, svol. 14, no. 2, pp. 1914-1917, 2004.
[21] N.E. Huang, Z. Shen, S.R. Long, "The empirical mode decomposition and Hilbert spectrum for nonlinear and nonstationary time series analysis," *Proceedings of the Royal Society of London A*, vol. 454, pp. 903-995, 1998.
[22] Jia Jide, Wu Chunzhi, Jia Xiangyu, et al, "A Time-Frequency Asnalysis Method Suitable for Engine Vibration Signals," *Automotive Engineering*, vol. 39, no. 1, pp. 97-101, 2017.
[23] R. Yan, R.X. Gao, "Hilbert-huang transform-based vibration signal analysis for machine health monitoring," *IEEE Transactions on Instrumentation And Measurement*, vol. 55, no. 6, pp. 2320- 2329, 2006.
[24] J. He, Z. Yu, R. Zeng, and B. Zhang, "Vibration and audible noise characteristics of AC transformer caused by HVDC system under monopole operation," *IEEE Transactions on Power Delivery*, vol. 27, no. 4, pp. 1835-1842, 2012.

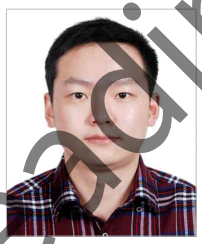

Xingmou Liu He received Ph.D degree in electrical engineering from Chongqing University. His research interests are electromagnetic field calculation and electrical equipment monitoring.

Yongming Yang He received Ph.D degree in electrical engineering from Chongqing University. Her research interests are electromagnetic equipment analysis and monitoring.

Yichen Huang He received her master degree in electrical engineering from Chongqing University. His research interests are electrical construction and safety management.